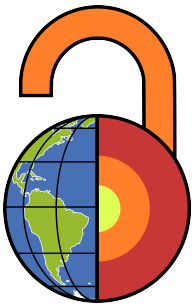

From Points to Predictions: Data Curation for Geospatial Machine Learning

Authors

Louis Saumier
School of Earth and Ocean Sciences, University of Victoria, Victoria, Canada
Email: lsaumier@uvic.ca
ORCID: 0009-0002-3287-9227

Joe R. Melton
Climate Research Division, Environment and Climate Change Canada, Victoria, Canada
Email: joe.melton@ec.gc.ca
ORCID: 0000-0002-9414-064X

Scott Winton
Environmental Studies, University of California Santa Cruz, Santa Cruz, USA
Email: scwinton@ucsc.edu
ORCID: 0000-0002-9048-9342

Preprint status

This manuscript is a **non-peer-reviewed preprint** submitted to **EarthArXiv**.
The manuscript has been submitted for peer review to **Machine Learning: Earth** and is currently under consideration.

This coversheet is intended to serve as page 1 of the EarthArXiv submission.

From Points to Predictions: Data Curation for Geospatial Machine Learning

Louis Saumier[1], Joe R. Melton[2,1], Scott Winton[3]

[1]School of Earth and Ocean Sciences, University of Victoria
[2]Climate Research Division, Environment and Climate Change Canada
[3]University of California Santa Cruz

The quality of training datasets can have a large impact on Machine Learning (ML) models, yet this aspect of the pipeline frequently receives less scrutiny than it should. In the context of geospatial mapping from point-scale field data, quality control strategies to remove erroneous or misleading data can be applied prior to model training to improve performance. However, such strategies and their resulting impact are rarely reported, compared to extensive discussions of model selection and tuning. To investigate the potential for spatial data error correction, we examine the case of peatland mapping from peat core samples. We assess several curation strategies and compare fully automated filters against filters that require monitoring by domain experts. We find that cleaning strategies based on location precision and landcover classification filtering to detect mismatches can significantly improve performance metrics. We also find that blind reliance on fully automated classification may lead to worse results. Despite the additional effort required, we conclude that manual spatial data quality control processes are an important component of large-scale spatial modelling and discuss recommended approaches to scale them effectively for large datasets.

Keywords: geospatial machine learning; data-centric machine learning; peatland mapping; location accuracy; landcover filtering

1 Introduction

Environmental variables are often most readily observable at scales that differ substantially from the spatial scales required to address large-scale ecological and environmental questions. Critical subsurface and soil properties–including soil chemistry, physics, and biology, as well as groundwater and bedrock geology–along with key biogeochemical processes such as methane emissions, N_2O fluxes, phosphorus availability, and decomposition rates, are typically measurable only at point scales through direct field sampling. However, understanding these variables across broader spatial extents is essential for addressing fundamental questions about land surface responses to future climate change, deforestation, and other environmental pressures. To bridge this scale gap, point-scale field data can be integrated with spatially continuous environmental covariates through predictive modeling approaches, generating spatially explicit maps that enable landscape-to regional-scale inference and analysis.

Emails: lsaumier@uvic.ca, joe.melton@ec.gc.ca, scwinton@ucsc.edu.

An example is the mapping of soil profile types (Wadoux, Minasny and McBratney, 2020), where point-scale field measurements are readily available in open-source repositories (e.g., Batjes, Ribeiro and Oostrum, 2020). Researchers have leveraged these databases to generate predictive maps serving diverse applications (Poggio *et al.*, 2021; Turek *et al.*, 2023). The proliferation of machine learning (ML) has made it increasingly straightforward to train predictive models by using data aggregated from multiple sources. However, ML practitioners often prioritize model architecture comparisons and hyperparameter optimization over examining how data characteristics influence model outputs (Aroyo *et al.*, 2022; Roscher *et al.*, 2024). This emphasis on algorithmic refinement overlooks the potentially substantial–yet underexplored–impact of data quality and composition on predictive performance (Li *et al.*, 2021).

To demonstrate the impact of data curation on mapping of point-scale environmental variables, we examine peatlands as a case study. Peatlands are globally important carbon (Jackson *et al.*, 2017) and freshwater stores (Joosten and Clarke, 2002). Despite covering only about 3% of the land surface (Xu *et al.*, 2018; Melton *et al.*, 2022), they are estimated to contain around a third of soil organic carbon– exceeding the carbon stored as biomass in all forests combined (Unep, 2022). While their ecological and climatic importance is widely acknowledged (Gorham, 1991; Turetsky *et al.*, 2015; Unep, 2022), peatlands remain poorly mapped worldwide, with particularly significant knowledge gaps in tropical regions (Dargie *et al.*, 2017; Girkin *et al.*, 2022; Minasny *et al.*, 2023; Hastie *et al.*, 2024; Winton *et al.*, 2025; Austin *et al.*, 2025).

Given these knowledge gaps, peatland mapping has been the focus of numerous research initiatives over recent years (Xu *et al.*, 2018; Minasny *et al.*, 2019, 2023; Melton *et al.*, 2022). Recent efforts have increasingly employed ML models to "fill in the gaps" and produce regional to global maps. These models integrate environmental predictors hypothesized to relate to peatland occurrence and characteristics – including climatic, vegetation, topographic, and hydrological indicators – with various combinations of existing peatland maps and/or peat soil core data to predict peatland extent and depth (Hugelius *et al.*, 2020; Melton *et al.*, 2022; Musthofa *et al.*, 2022; Fiantis *et al.*, 2023; Minasny *et al.*, 2023; Ivanovs, Haberl and Melniks, 2024; Cha *et al.*, 2024; Hastie *et al.*, 2024; Pontone *et al.*, 2024; Pohjankukka *et al.*, 2025; Lara *et al.*, 2025; Pan *et al.*, 2025; Jade Skye, J. R. Melton, *et al.*, 2025; Widyastuti *et al.*, 2025). Despite the extensive efforts in this area, relatively little attention has been devoted to the effects of point-scale data quality and preprocessing on ML model performance. While some studies do mention filtering their point-scale data (e.g., Pohjankukka *et al.*, 2025; Lara *et al.*, 2025; Pan *et al.*, 2025), such approaches remain uncommon. Critically, none quantify the effects of data cleaning on the ML models – i.e. none present comparative results obtained with and without data filters applied to assess whether the effort to quality control the data leads to better models.

There is good reason to suspect that data curation measures applied to peatland point-scale data would yield significant benefits. Many peat soil cores collated in previous studies (e.g., Treat *et al.*, 2017; Hugelius *et al.*, 2020) or as part of peat databases (e.g., J. Skye *et al.*, 2025) have been collected across multiple decades, with some dating as early as 1905 (personal communication April Dalton, 2025), often with unknown or poorly documented sampling dates. Furthermore, the sampling equipment and methods used reflect the available technology of their time and region, leading to older data frequently suffering from reduced spatial precision. As well, some data were collected during field surveys where the mapping of peatland depth or extent was a

secondary consideration, potentially compromising data quality for mapping applications. Of course, all point-scale data also remains susceptible to simple errors such as being incorrectly recorded or possessing reduced precision coordinates. As peatlands are susceptible to human activities and natural forces, a peatland may have significantly changed since the time of sampling – for example, following drainage for agriculture (Fluet-Chouinard *et al.*, 2023), overgrazing (Li *et al.*, 2018), peat extraction for fuel, flooding by construction of roads or dams, burying by construction of infrastructure, or wildfire events. Some soil cores also stem from pre-construction geotechnical surveys, in which case they may not faithfully represent the current state of the sampling site.

In a recent review, (Roscher *et al.*, 2024) emphasize the importance of treating data quality rigorously instead of focusing on data quantity in training datasets. They also highlight the need for developing automated data cleaning procedures. We draw inspiration from their data-centric framework, but also investigate whether leveraging domain expertise is essential for achieving optimal results. To understand this, and inform current and future peatland mapping efforts, we test how combining automated or semi-automated filtering with expert visual validation affects ML model performance when mapping peat soil cores. The point-scale data we use for our experiments are from Peat-DBase (J. Skye *et al.*, 2025; Jade Skye, J. Melton, *et al.*, 2025), a collection of peat soil cores gathered from published and unpublished compilations and regional data sources. The cores have latitude and longitude coordinates recorded in decimal format along with a measurement of peat depth in centimeters for each set of coordinates. Recognizing that interdisciplinary collaborations often involve machine learning specialists lacking domain-specific knowledge to accurately filter datapoints and peatland scientists without extensive programming experience, we demonstrate how user-friendly technologies can bridge this expertise gap.

Our paper is organized as follows. Sections 2.1 and 2.2 presents the data and discuss key issues and challenges encountered. Section 2.3 introduces different curation strategies as potential solutions to these challenges, while Section 3 demonstrates their impact on a ML model performance through comprehensive numerical experiments. This is followed by a discussion of those numerical results in Section 4. Finally, Section 5 presents future related work while Section 6 synthesizes the insights gained and provides some practical recommendations for scientists developing geospatial maps of environmental variables.

2 Methods

2.1 Peat Data

We use version 0.9 of Peat-DBase (J. Skye *et al.*, 2025; Jade Skye, J. Melton, *et al.*, 2025), which includes everything from version 1.0 of the database except for the Scotland Peatland Action data (Scottish Government, 2025). We leverage Peat-DBase to train a machine learning (ML) model that predicts peatland presence across a global 5 arc-minute grid. This relatively coarse-resolution approach serves as a computationally efficient screening tool, identifying candidate cells for subsequent fine-scale analysis of peatland presence and depth. Given that this coarse

grid represents an initial filtering stage designed to reduce computational demands for high-resolution peatland mapping, we prioritize high recall (proportion of true peatland samples captured by the model) over precision (proportion of predicted peatland samples that actually contain peat)– aiming to capture the vast majority of existing peatlands while accepting a higher rate of false positives.

Given that we want to predict peatland presence, we convert the Peat-DBase depth measurements into binary indicators. We then remove any duplicates that come from multiple depth measurements at the same geographical location and we are left with 32 736 individual peat presence measurements. We note that it is important to remove the duplicates as they can become an additional source of bias for the model (Sarracino and Mikucka, 2017). In order to properly train the ML model to understand peat absence, Peat-DBase contains 94 615 non-peat soil points taken from the World Soil Information Service (WoSIS) dataset (Batjes, Ribeiro and Oostrum, 2020).

Hereafter, we refer to peat core samples obtained from actual field measurements of peatlands as *peat-study* points (or cluster of points). We note that some of those data points may still have a reported depth of zero depending on study protocols and are thus associated with peat absence when converted to binary indicators. In contrast, we use the term *non-peat-study* points (or cluster of points) to designate mineral soil samples added to the database to support ML model training. These data points were collected from the WoSIS database (Batjes, Ribeiro and Oostrum, 2020) and were all assigned a peat depth of zero, hence also associated with peat absence.

Since the peat data points are obtained from diverse sources and were collected for various purposes, they exhibit varying levels of reliability that can negatively affect ML model performance. We now explore the key data quality issues present in Peat-DBase that can significantly impact modeling results.

2.2 Issues with the Data

2.2.1 Coordinate (Im)Precision

Table 1: Number of entries in Peat-DBase v.0.9 below different coordinate precision thresholds and their associated spatial uncertainty at the equator (32 706 points remaining after removing 30 clustering outliers - see Appendix A).

Significant Digits	Number of Entries	Uncertainty	Example
0	254	111 km	(57.0, -75.0)
1	988	11.1 km	(43.0, -77.8)
2	1699	1.11 km	(51.17, -100.25)
3	1584	111 m	(49.133, -90.75)
4	2150	11.1 m	(45.3975, -93.1891)
5	6352	1.11 m	(41.00945, -82.7325)
6	19679	11.1 cm	(54.12449, 7.745455)

The first and perhaps most impactful data quality concern is coordinate precision. Data points in Peat-DBase exhibit substantial variation in positional recorded precision. Table 1 shows the number of coordinates recorded with d or fewer significant digits in both latitude and longitude for $d \in \{0, 1, \ldots, 6\}$, along with the associated spatial uncertainty at the equator. While this uncertainty varies with latitude, these values provide a reasonable estimate of potential error magnitude.

Several factors may explain why some coordinates are recorded with limited precision:

- [**Equipment age**] Samples collected many years ago using less sophisticated positioning equipment.
- [**Collection purpose**] Data not intended for high-precision mapping applications, making exact coordinates less critical during sample collection.
- [**Privacy protection**] Coordinates deliberately obfuscated to protect local population privacy or sensitivites.
- [**Recording errors**] Inadvertent reduction in precision during data collection or entry.
- [**Chance**] Legitimate measurements that happen to terminate with zeros.

While determining the specific cause of low precision for individual datapoints is challenging, we can evaluate the impact of excluding such points from training datasets. We investigate this filtering approach and its effects on ML model performance in Section 3.1.2. Additionally, coordinate system conversions (e.g., from Degrees/Minutes/Seconds to Decimal Degrees) may alter the apparent number of significant digits without changing actual measurement precision, as discussed further in Section 4.

2.2.2 Entry Errors

Entry errors are unavoidable yet difficult to detect. For example, preliminary exploration using Google Earth revealed a datapoint with coordinates (-9.4655° latitude, 77.3785° longitude), which is located in the Indian Ocean. Further investigation revealed this data point belonged to a group of soil cores sampled in South America, suggesting an incorrect longitude sign (whereby a positive longitude indicates degrees West and a positive latitude degrees North). We discuss methods to detect and remove such errors in the following sections using automated filters combined with geospatial software functionalities.

2.2.3 Dated Measurements

Some data in Peat-DBase originates from studies conducted decades ago. Beyond the potentially lower precision of older sampling instruments, many peatlands have been significantly altered by anthropogenic activities (e.g. construction, drainage) or natural disturbances (e.g. fires, landslides). Moreover, tracing the collection date of individual cores is often difficult or impossible. Determining whether historical cores represent current peatland conditions can be addressed using historical imagery, as demonstrated using remotely sensed imagery in Figure 1.

(a) (b)

Figure 1: Peat core locations on an island in northern Norway for (a) 1985 imagery and (b) 2025 imagery as an example of dated measurements. The peat cores were likely sampled before this industrial complex was built.

2.2.4 Sampling Bias

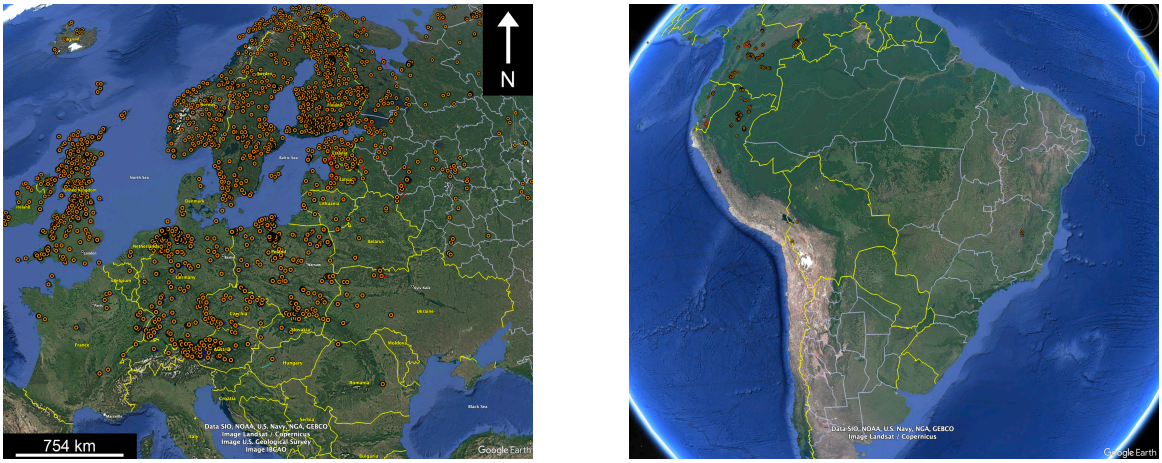

(a) (b)

Figure 2: Distribution of peat cores from Peat-DBase version 0.9 in Europe (a) and South America (b). Even when taking into account the smaller areal extent of tropical peatlands, the peat cores available are highly biased toward the high latitudes.

Sampling bias presents a significant challenge for the creation of global peatland maps. While northern latitude peatlands have been extensively sampled, tropical peatlands have comparatively few available cores. Indeed, some tropical peat deposits have only been discovered within

the last few years (e.g., Dargie *et al.*, 2017; Winton *et al.*, 2025), demonstrating the data scarcity in these regions. The result is a database skewed toward northern latitudes, as illustrated in Figure 2. This geographic bias must be addressed to avoid developing models that perform well only at northern latitudes.

2.3 Data Curation

In order to address the data quality issues raised in the previous section, we present here our curation methodology. We note that sampling bias is not specifically addressed through data curation, but rather through clustering the data and assigning weights to individual data points, thereby balancing the loss function during model training. Details for the clustering procedure are presented in Appendix A.

2.3.1 Expert-Based Manual Filtering

Relying solely on expert-based manual cleaning is often impractical given database sizes, yet fully automated procedures can miss errors obvious to human observers. Accessible geospatial visualization tools can enable researchers to dynamically explore databases and identify measurements that immediately appear incorrect. Accessibility is crucial when machine learning specialists collaborate with domain experts (peatland scientists in our case) to identify data points requiring removal from training datasets.

There are many differet geospatial visualization software available that can be used by researchers to filter data points. Some are free to use (e.g. QGIS, Google Earth and Google Earth Engine), while others require a paid subscription either for the basic version, for higher tiers only, or for commercial use (e.g. ArcGIS, CARTO, Mapbox). Some are available only on desktop (e.g., QGIS, ArcGIS Pro, Google Earth Pro), while others can be used on a web browser without installation (e.g., ArcGIS Online, Google Earth Web and Google Earth Engine, CARTO, Mapbox). Some require no coding and minimal training to use (e.g., ArcGIS Online, Google Earth Pro and Web, Mapbox Studio, CARTO) while others either need users to know how to code, or have a steeper learning curve (e.g., QGIS, ArcGIS Pro, Google Earth Engine, Mapbox GL JS). We note that there are many more such geospatial visualization tools not listed here, including libraries such as GeoPandas, Leaflet and MapLibre.

Researchers have to select a tool that is best suited for their needs based on the options available. For our study, we chose Google Earth for a few reasons. First, Google Earth's web platform facilitates project sharing among multiple collaborators, allowing team members to flag problematic points as needed. Second, the free desktop version enables creation of data "tours"–systematic workflows for reviewing points within pre-specified categories, with functionality to pause and examine locations in detail. Third, it is accessible for free anywhere in the world, an important consideration when the peatland field scientists used as expert assessors can be based in countries lacking extensive computing infrastructure. We incorporated geographical coordinates and peat depth as text fields for each data point, added error bars indicating positional uncertainty

based on recorded significant digits, and overlayed 5 arc-minute grid cells to visualize how coordinate uncertainty affects grid-level predictions. These features are illustrated in the images presented in subsequent sections.

2.3.2 Significant Digits Filtering

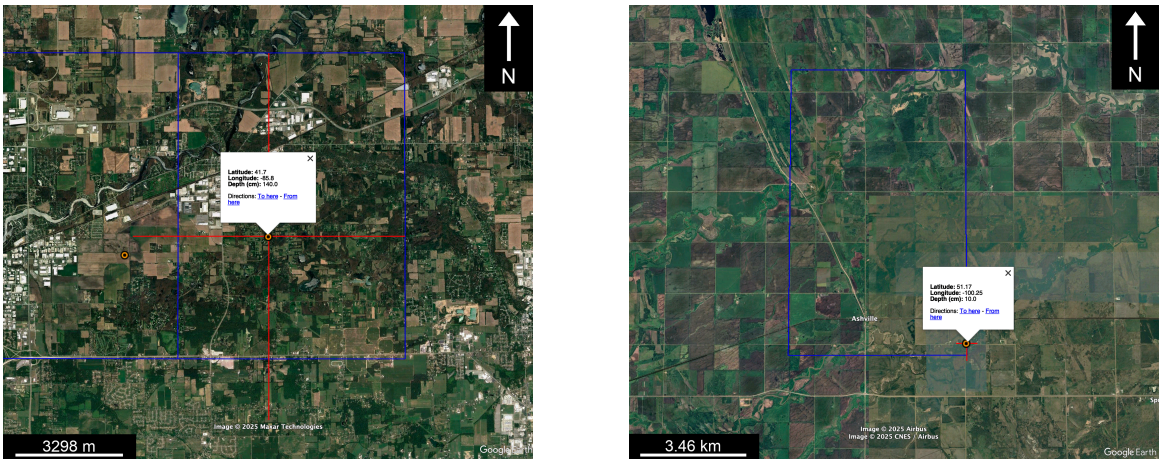

(a) (b)

Figure 3: Examples of the impact of precisional uncertainty for peat cores with: (a) one significant digit in Northern Indiana, USA and (b) two significant digits in Manitoba, Canada. The red lines indicate the positional uncertainty while the blue lines show the borders of the global 5 arc-minute grid. These two cores are low-precision points that should likely be removed from training. In the Northern Indiana case, we see that the uncertainty in the coordinates are large enough that the point could realistically belong to a different grid cell, even if the datapoint itself is located close to the center of its closest 5 arc-minute cell. We may also have a similar issue in the Manitoba case, despite the higher precision measurements.

Coordinate precision significantly influences model quality, with effects varying by predictive grid resolution. Points with large positional uncertainty due to few recorded significant digits have higher probability of assignment to incorrect grid cells, as illustrated in Figure 3. When using a 5 arc-minute grid, points with 0 or 1 significant digits (e.g. $50°$ N or $50.1°$ N) may degrade ML model performance since their uncertainty exceeds grid cell dimensions (see Table 1). However, even points with higher precision can be erroneously assigned when located near cell boundaries. This issue is not unknown; (Batjes, Ribeiro and Oostrum, 2020) emphasize that scientists using soil cores for mapping should carefully consider coordinate accuracy, as low precision can associate datapoints with incorrect predictor values.

To address this we introduce a significant digits filter. This filter operates by removing all data points (both peat-study and non-peat-study points) with fewer than d significant digits before training the ML model. We implement two variants of this filter: one that removes data points

where both latitude and longitude have d or fewer significant digits (AND-d filter), and another that removes data points where either latitude or longitude has d or fewer significant digits (OR-d filter). We validate the performance of both filters through numerical experiments in subsequent sections and provide practical recommendations for addressing coordinate uncertainty.

Additionally, when filtering data to eliminate points with poor geographical precision, we must consider the original coordinate system used for data recording, potential conversions between systems, and precision loss during conversion. For example, many peat soil core coordinates were likely recorded in Degrees/Minutes/Seconds (DMS) rather than Decimal Degrees (DD). Applying a filter to coordinates converted from DMS to DD may inadvertently retain low-precision points. Indeed, a latitude of 41°20′ in DMS (whereby the seconds were not recorded) converts to 41.333333° DD (retaining 6 decimals), which may go unnoticed when using automated cleaning procedures, despite having a positional uncertainty of 1.85 km at the equator (equivalent to 1 arcminute). This will also be investigated in our experiments.

2.3.3 Landcover Filtering

While the clustering procedure outlined in Appendix A used the ESA landcover product to cluster non-peat-study data points for loss function weighting, this classification can serve an additional purpose: filtering peat-study data. Applying landcover classification to peat data points can identify measurements not actually located on peatlands, including erroneous datapoints or outdated data points that no longer represent current land cover or land use. Table 2 presents the classification results for our peat data.

Table 2: Number of peat-study data points per ESA landcover class (32 689 in total). Notably, 17 data points returned no landcover class due to oceanic locations too distant from land for ESA coverage, indicating candidates for removal from training datasets.

ESA Landcover Class	Number of Data Points Identified
Bare / sparse vegetation	121
Built-up	235
Cropland	267
Grassland	9153
Herbaceous wetland	10649
Mangroves	160
Moss and lichen	241
Permanent water	659
Shrubland	310
Snow and ice	15
Tree cover	10879

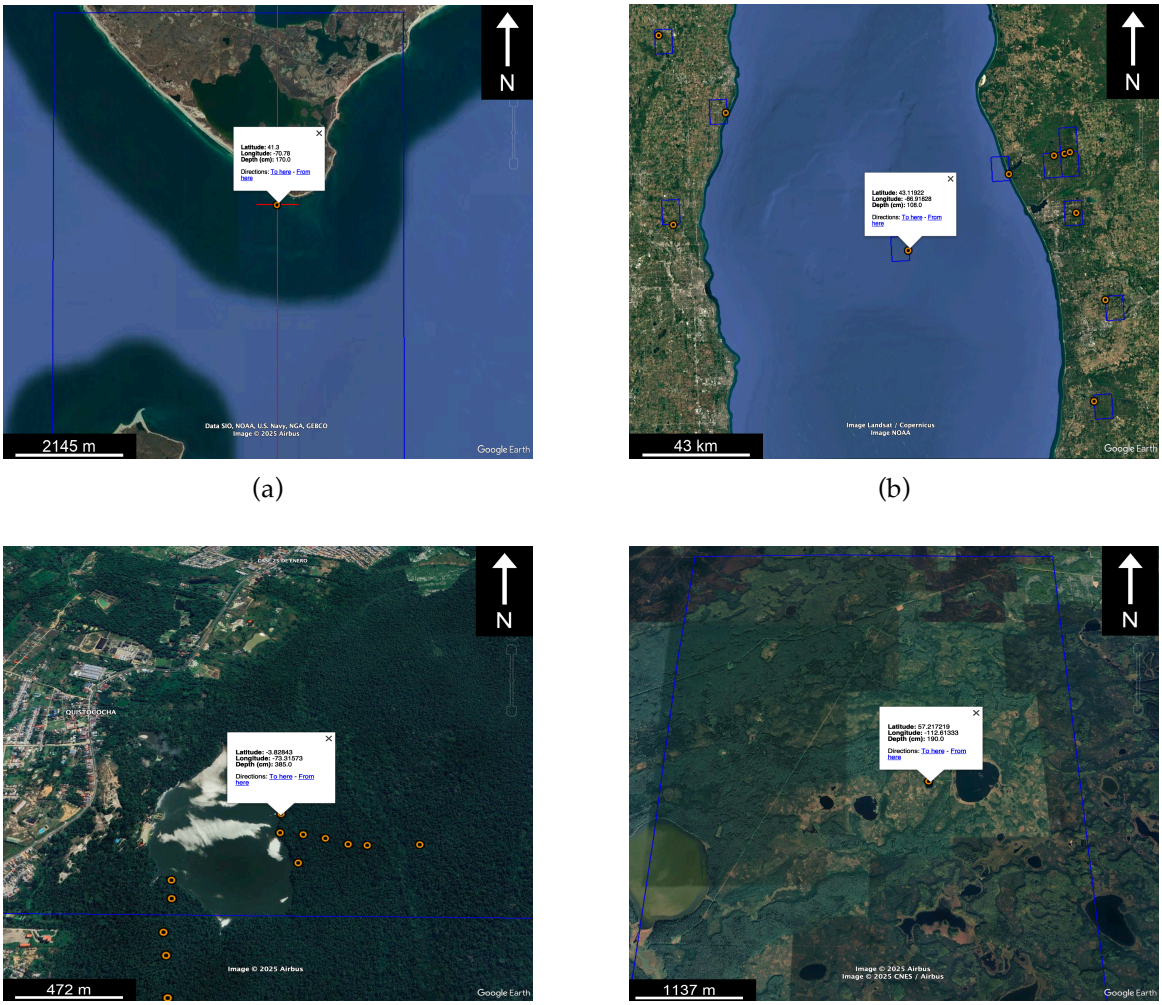

Figure 4: Examples of peat core locations classified as the ESA land cover class "Permanent Water" with varying coordinate precision and suggested utility for training: (a) Near Rhode Island, USA (low precision, excluded from training); (b) Lake Michigan, USA (high precision, excluded from training); (c) Loreto, Peru (on lake edge, retained for training); and (d) Alberta, Canada (retained for training).

Examining the classifications reveals that some datapoints may require filtering before ML model training. Figure 4 shows data points classified as the ESA land cover class "Permanent Water" that could confuse models due to precision issues or entry errors. However, not all require elimination. The Peru example (Figure 4c) shows a datapoint at a lake edge, which is likely sufficiently close to surrounding peatland to warrant retention. Similarly, the Alberta data point (Figure 4d) falls within a small lake but occupies a relatively uniform grid cell that appears to contain peatlands, which could be used to justify its inclusion. While for all cases shown in Figure 4 the samples did in fact appear to be located in permanent water, such landcover classification prod-

ucts can still contain errors, further reinforcing the need to review those points manually. Figure 5 presents two "Croplands" land cover class examples with different implications. The urban cropland location in Figure 5a suggests the soil core sample is no longer representing a peatland ecosystem. On the other hand, Figure 5b presents a core located on a small cropland, but situated near a large peatland nature reserve contained within the same grid cell. For these reasons, the first sample is likely best removed prior to training while the second can be retained.

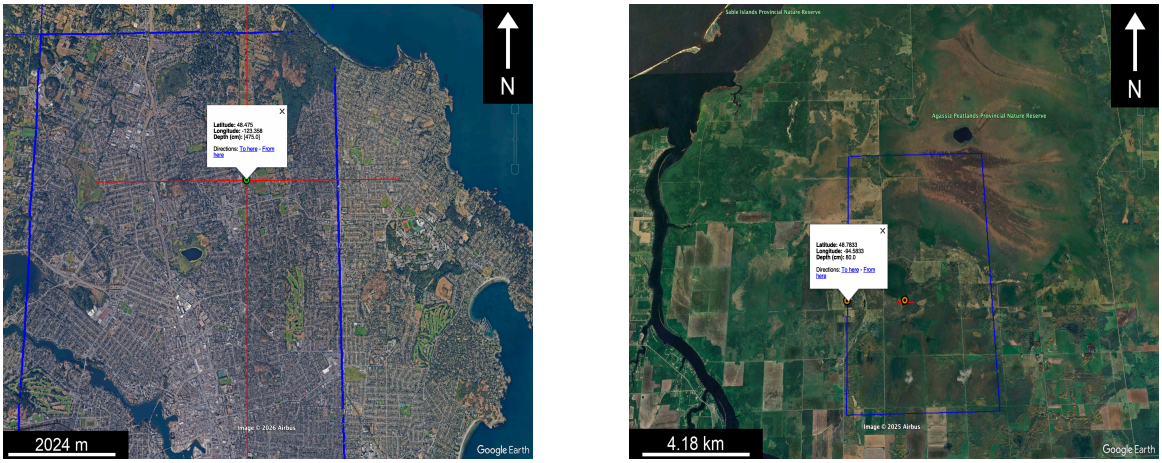

(a) (b)

Figure 5: Two examples of locations classified as the ESA land cover class "Cropland": (a) an urban cropland in Victoria, Canada and (b) a small cropland within large peatland nature reserve in Ontario, Canada.

Applying landcover filters to peat-study points reveals sites that may not accurately represent peatlands. It is arguably reasonable to exclude points falling within "Built-Up", "Croplands", "Permanent Water", or "Snow and Ice" classes. However, as demonstrated by this section's examples, not all data within these categories warrant exclusion. Indeed, many grid cells capture mixed environments or transitional zones where peatlands are adjacent to other landcover types. In the case of croplands, genuine peatlands may still be present and under agricultural use (a common situation in Europe); however, some cropland-associated peat cores are located in highly modified or marginal settings that may be unsuitable for ML model training, as demonstrated by the Victoria example above. These cases may benefit from additional review by an expert with domain knowledge and contextual understanding of the landscape, allowing them to judge whether they are representative for ML model training, even if the landcover classification is ambiguous. To verify the importance of these considerations, we investigate two filtering strategies:

- [**landcover-auto**] Automatic removal of all data points falling within the "Permanent Water", "Croplands", "Built-up", or "Snow and Ice" categories,
- [**landcover-manual**] Manual inspection of data points falling within these four categories, removing only those deemed erroneous or inappropriate for training via expert judgement.

For the manual filtering approach, we conducted systematic quality assessment using Google Earth. We generated separate KML files for each of the four potentially problematic landcover types and used Google Earth's tour feature to systematically examine each location. This process involved inspecting 1,176 locations, of which 208 were flagged for removal. During this manual review, we also identified numerous zero-depth measurements in the Congo Basin that would likely introduce noise when training on a 5 arcminute grid resolution, and these were subsequently removed as well.

2.4 Model

To assess the impact of the various cleaning procedures on the predicted results, we use LightGBM– a gradient-boosting ML algorithm –with a model framework similar to the one employed in (Melton *et al.*, 2022). The model is configured as a binary classifier to predict peat presence on a coarse 5 arc-minutes grid, using a group of 20 predictors selected for their high relative importance. We also employ a Staggered Block-Leave-One-Out Cross-Validation (SBLOO-CV) scheme to address the spatial autocorrelation of the residuals inherent to geospatial ML. Full implementation details are provided in Appendix B.

3 Results

3.1 Effect of Cleaning Procedures

3.1.1 No Filtering

We establish our baseline using results from the algorithm trained on clustered but unfiltered data, removing only clustering outliers and non-peat-study points lacking valid landcover classification. Figure 6 shows our model's performance on this baseline dataset. The plotted performance metrics (Figure 6a) reveal that the accuracy-recall intersection can provide an optimal threshold location for classifying peatland presence (this is a probability threshold that determines what cells will be considered to potentially contain peatlands). At this point of intersection, both recall and accuracy are high, while precision and F1-score transition from rapid change to gradual improvement as the probability threshold increases. The F1-score effectively plateaus at this value, increasing slightly before beginning to decline at higher thresholds. We therefore adopt the accuracy-recall intersection as our threshold for all subsequent tests. Following our SBLOO-CV approach, this threshold is selected based on validation data performance and can then be applied to the full model for predicting peat presence on test sets or globally.

3.1.2 Significant Digits Filter

Having established a baseline, we can now evaluate the impact of a significant digits filter. The effect of various versions of this pre-training filter are presented in Figures 7, 8, and 9. The AND-

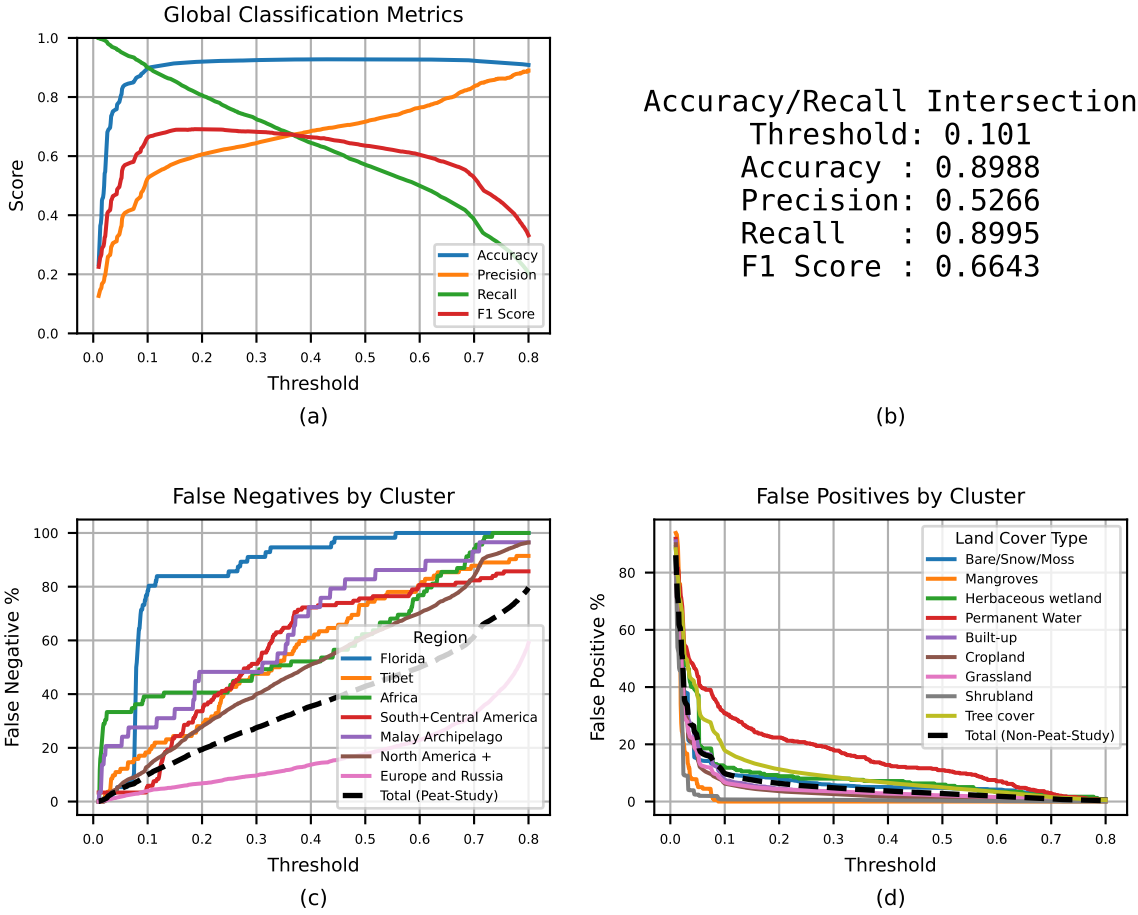

Figure 6: Global and cluster-wise performance metrics across thresholds for the unfiltered dataset. *Threshold* is defined as the probability cutoff used to determine which grid cells will be considered to potentially contain peatlands and thus be further investigated. Panel a shows the accuracy, recall, precision and F1 score as a function of the threshold value, based on validation sets results obtained using SBLOO CV - see Appendix B.3. Panel b represents all performance metrics values at the intersection point between the accuracy and recall curves. Finally, panel c shows the false negative rate across peat-study clusters whereas panel d displays the same results but for the non-peat-study clusters.

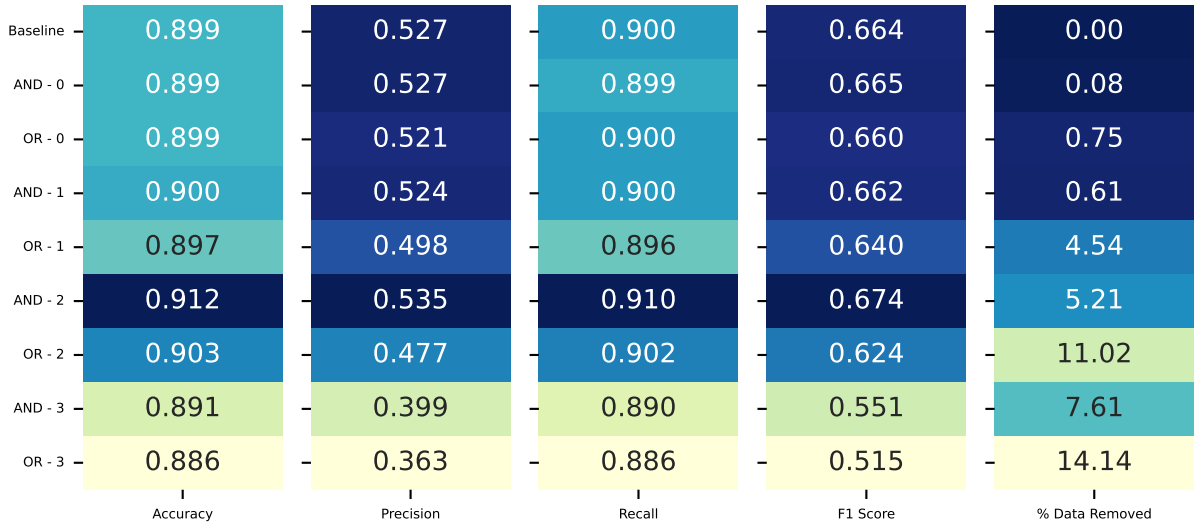

Figure 7: Comparison of classification performance metrics (accuracy, precision, recall, F1-score) across different types of precision filters, as defined in Section 2.3.2. Darker colours represent more desirable results (improved performance metrics and smaller proportion of discarded samples).

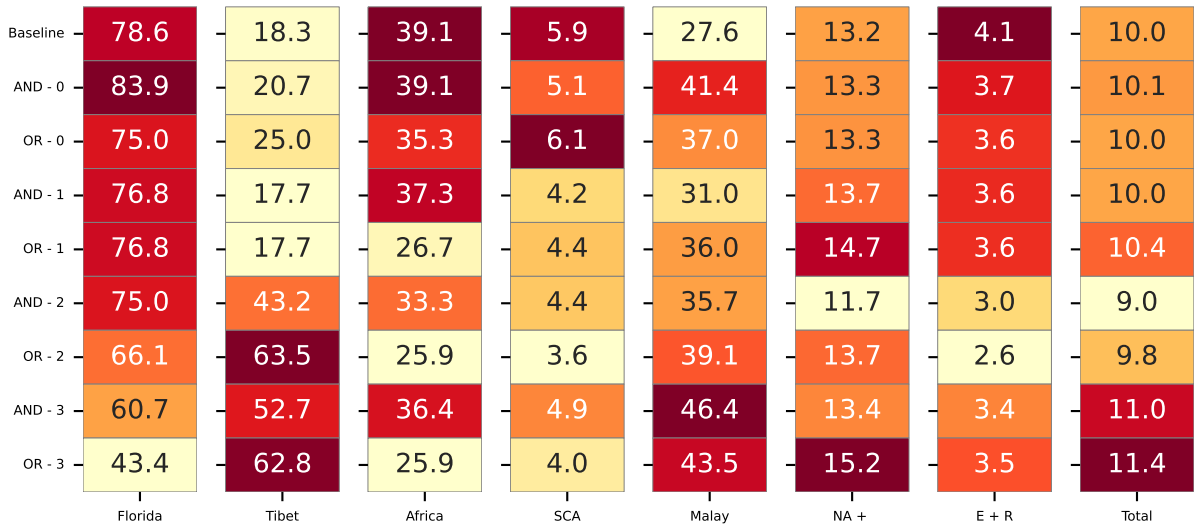

Figure 8: False negative rate (% of peat points missed) per peat-study cluster across filtering strategies, as defined in Section 2.3.2. Lighter colours represent more desirable results (reduced false negative rate).

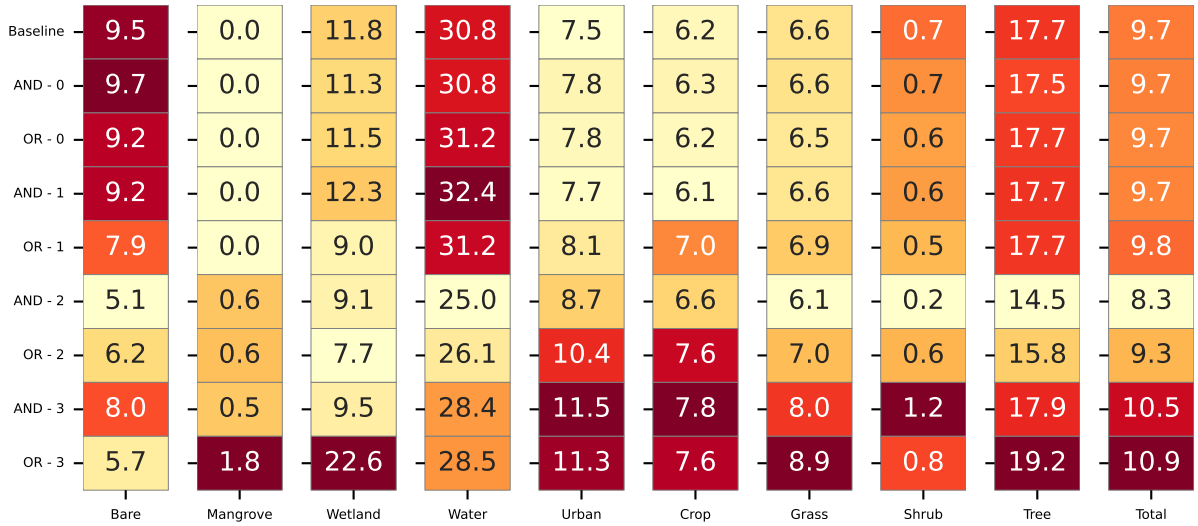

Figure 9: False positive rate (% of non-peat points incorrectly predicted as peat) per non-peat-study cluster across filtering strategies, as defined in Section 2.3.2. Lighter colours represent more desirable results (reduced false positive rate).

2 filter yields the best results, with significant improvements across all metrics. We also tested whether different predictor variable selections would alter the optimal filter choice. These analyses, presented in Appendix C, demonstrate that predictor selection does not appear to influence which filter performs best. Finally, given the substantial number of soil cores with 0-2 significant digits in both coordinates (2,957 data points in total), individual manual verification was not performed. However, we will examine the impact of approaches involving expert manual assessment for landcover-based filtering in the following section.

3.1.3 Landcover Filter

Next, we experiment with landcover-based filtering as an alternative method for removing problematic datapoints prior to model training. The results for both landcover-auto and landcover-manual filters are presented in Figures 10, 11, and 12. We also evaluate the performance when combining landcover filters with the significant digits approach, using AND-2 as the optimal filter from the previous section.

3.2 Effect on a Global Map

As a final assessment, we evaluate the impact of data filtering on global peatland predictions generated by our ML model. We apply the optimal filter combination identified in our numerical experiments—the AND-2 and landcover-manual filters—to the complete database, train the model on the remaining data points, and calibrate probabilities using Platt scaling (Böken, 2021)

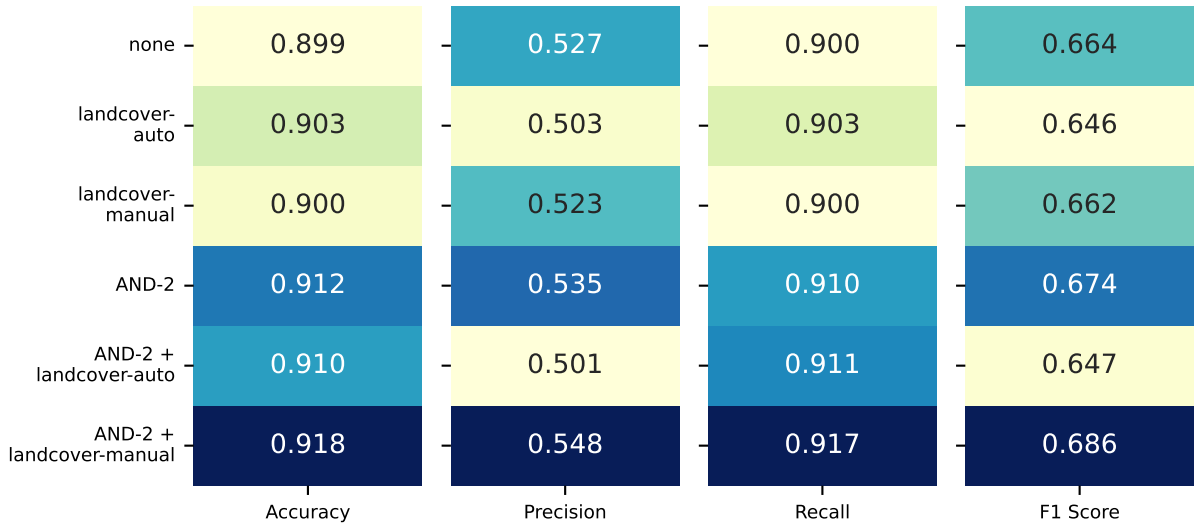

Figure 10: Comparison of classification performance metrics (Accuracy, Precision, Recall, F1) across different filtering strategies, as defined in Section 2.3.2. Darker colours represent more desirable results (improved performance metrics).

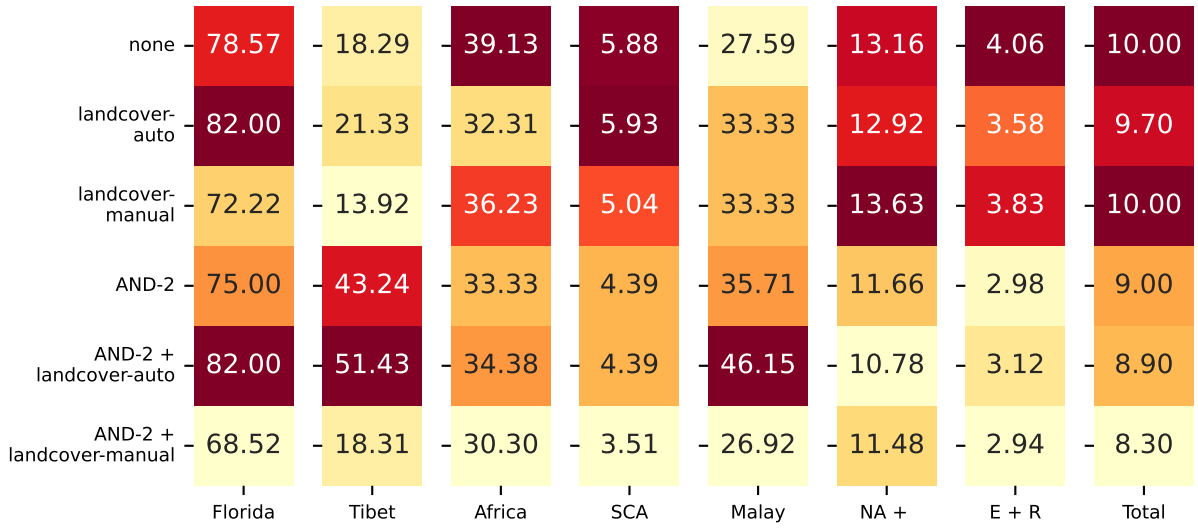

Figure 11: False negative rate (% of peat points missed) per peat-study cluster across filtering strategies, as defined in Section 2.3.2. Lighter colours represent more desirable results (reduced false negative rate).

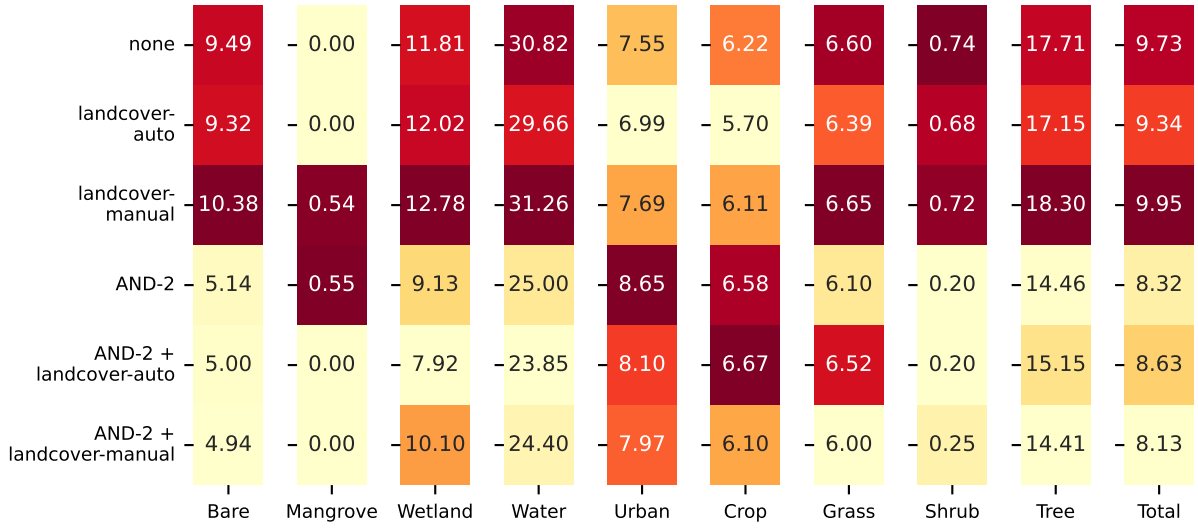

Figure 12: False positive rate (% of non-peat points incorrectly predicted as peat) per non-peat-study cluster across filtering strategies, as defined in Section 2.3.2. Lighter colours represent more desirable results (reduced false positive rate).

with parameters derived from validation sets during SBLOO-CV (see Appendix B). The resulting model is then used to predict peat presence across a global 5 arcminute grid.

The filtering approach produces a substantial difference in global predictions. Of the 7 784 640 grid cells, 32.41% were classified as containing peat using the unfiltered baseline dataset, compared to 28.83% when applying our combined filters. This represents a reduction of 3.58 percentage points, or 278 953 fewer grid cells predicted to contain peat.

4 Discussion

4.1 Model Performance

From the results shown in Figure 6, at the selected threshold, accuracy and recall are both at roughly 90%, while precision is considerably lower at 52.7%. This trade-off is intentional, as we prioritize minimizing false negatives to capture the majority of peatlands rather than maximizing precision. However, the false negative rate varies substantially across clusters, which correlates with the density of available soil cores in each region (e.g. poorly sampled clusters such as the Malay Archipelago tend to exhibit higher false negative rates compared to clusters with more samples such as Europe and Russia). The apparent poor performance in the Florida cluster likely reflects an artifact of our SBLOO CV block selection methodology. As illustrated in Figure 2, most Florida points fall within a single CV region, meaning the model is never trained on Florida data when making predictions for that area. Given the unique composition of Florida peatlands (Dreschel *et al.*, 2017), requiring the model to predict peat presence without any regional training

data represents an overly conservative evaluation scenario. This can potentially be mitigated by selecting different boundaries for the SBLOO CV block and by collecting more data for that region.

Among non-peat-study clusters, the ESA land cover class "Permanent Water" cluster shows the highest false positive rate. This pattern is understandable given that peatlands are wetland ecosystems, and thus it can be challenging for a model to distinguish them from other water bodies. We also point out that this assumes the points designated as "Permanent Water" by the ESA classification are truly permanent water bodies, which is not guaranteed. In fact, the "Permanent Water" class contains any geographic areas that are covered by water for more than nine months per year (Zanaga *et al.*, 2022), and may therefore include some peatlands.

4.2 Filters Performance

The AND-2 filter, which removed all data points where both latitude and longitude have 2 or fewer significant digits, yields the best results. This is particularly noteworthy given our coarse 5-arcminute grid resolution: even removing points with only 2 significant digits–corresponding to a positional uncertainty of 1.11 km at the equator–substantially improves model performance. As illustrated in Figure 3, such imprecise coordinates can cause points to be assigned to incorrect grid cells when they fall near cell boundaries. Our results suggest this level of positional uncertainty is sufficient to appreciably degrade ML model performance.

Applying the AND-2 filter removes 5.21% of the datapoints and improves accuracy, recall, precision, and F1-score by approximately 1% each. The AND-1 filter produces minimal changes, likely due to the small proportion of points removed (0.61% of the data) compared to the AND-2 filter. Conversely, the OR-1 filter decreases the values of all four classification metrics. This degradation likely occurs because 1285 points in our database (3.9% of the data) have one coordinate recorded with high precision (2 or more significant digits) while the other has only 0-1 significant digits. Such points are more likely to represent accurate measurements that coincidentally fall at locations where one coordinate appears imprecise, rather than genuinely low-quality positional data where both coordinates have few decimal places. In fact, computing the probability of these points occuring at random given the size of our database, we would expect that about 360 of the 1285 points have accurate coordinates that simply happen to have a lower number of non-zero significant digits in one of their coordinates, which is a significant ratio of the points removed by OR-1.

However, the AND-2 filter does not uniformly improve performance across all clusters. The false negative rate actually increases for the Tibetan Highlands and Malay Archipelago clusters. Both regions have relatively few sampled cores (135 and 388 cores, respectively), making them more sensitive to variations when training data are added or removed for predicting peat presence in these locations. In fact, the AND-2 filter removed 43% of the Tibetan Highlands data and 36% of the Malay Archipelago data, suggesting a relatively small percentage of reliable cores for those regions.

We investigated whether back-converting DD coordinates to DMS and filtering for low precision in both formats would improve results. However, this approach requires careful handling of

truncated decimals from recurring decimal fractions. For instance, converting 41.333333° DD to DMS yields 41°19′59.9988″, though the original measurement was more likely 41°20′00″. Our analysis (with results presented in Appendix D) found that such DMS filtering did not improve model performance. Nevertheless, this could represent a consideration when filtering similar databases of georeferenced data points.

When applying both significant digits and landcover filters, the best overall performance was achieved by selecting the AND-2 and landcover-manual filters. This approach improved each classification metric by approximately 2% and substantially reduced false negative rates across all clusters (1.7% overall improvement) except for Tibet, where performance remained stable. Similarly, false positive rates decreased across all landcover types (1.6% overall improvement), with only the "Urban (Built-up)" showing a slight increase (0.42%).

To put the 2% overall improvements in context, we refer to the work of Florek and Zagdański who present in a benchmark paper (Florek and Zagdański, 2023) the gains on accuracy obtained from tuning the hyperparameters for LightGBM (the ML model we use in this work - see Appendix B). Comparing the accuracy of the model tuned using standard Bayesian Optimization (Tree-structured Parzen Estimators) against the default model for 12 different binary classification datasets, they registered a mean and median improvement of 1.32% and 0.33%, respectively. While these gains vary considerably across the datasets they evaluated against, this suggests that the 2% improvement obtained in this work is comparable or greater than achievable gains from hyperparameter tuning.

Finally, we remark that the landcover-auto filter significantly degraded precision and F1-score while providing only marginal improvements in accuracy and recall. This highlights the risks of applying automatic landcover-based exclusions without careful evaluation. In addition, the landcover-manual filter alone produced limited improvements; substantial benefits were only observed when combined with the AND-2 filter, suggesting that these filtering approaches work synergistically rather than independently.

4.3 Global Performance

The relatively high peatland prediction percentages obtained are intentional, reflecting our methodology's design to maximize peatland detection sensitivity on a coarse grid, accepting higher false positive rates with the expectation that flagged areas will undergo subsequent fine-scale analysis using alternative methods. The coarse 5 arc-minute spatial resolution also contributes to these peatland prediction percentages, as grid cells may be classified as peat-containing even when peatlands occupy only a small fraction of the cell area.

The substantial reduction in predicted peat-containing cells (3.58%) demonstrates how effective data cleaning strategies can significantly influence ML model outcomes, underscoring the importance of systematic quality control in geospatial modeling applications. Given the improvement across all perfomance metrics when tested on validation sets (1.9%, 2.1%, 1.7% and 2.2% for accuracy, precision, recall and F1-score, respectively), it is reasonable to expect the impact of these changes to be positive.

5 Future Work

Future research should investigate how these cleaning procedures affect models across various grid resolutions. Filtering data points with limited decimal precision (e.g., 2 decimal precision is approximately 1 km uncertainty) likely impacts fine and coarse grids differently. We hypothesize that data cleaning benefits fine-resolution grids more substantially, as imprecise data points have greater impact on training values. Conversely, coarse grids may naturally dampen the effects of poor-quality data points through larger sample sizes per cell, where high-quality data points help attenuate noise from erroneous data points. In addition, landcover classes are more likely to be incorrect at coarser resolutions due to potentially containing pixels with many different landcover classes, and thus we also expect a filtering method based on landcover classification to perform better on finer grids. These hypotheses warrant further investigation.

6 Conclusion

Our study presents data filtering strategies for databases containing data points with geographical coordinates. Through careful pre-training data filtering, we achieved approximately 2% improvements in accuracy, recall, precision, and F1-score without comparing across different ML algorithms or hyperparameter tuning. This is in line with average performance gains that result from tuning LightGBM models (Florek and Zagdański, 2023), underscoring the significant impact of data quality within the context of peatland mapping. Our results demonstrate that half of this performance gain stemmed from filtering data points with low coordinate precision (few decimal places), while the remaining improvement came from a semi-automated process that relied upon expert assessment and removed data points within potentially unsuitable landcover types. Notably, automated landcover filtering without manual inspection decreased overall performance.

While manually reviewing hundreds or thousands of data points appears daunting, we demonstrate how accessible visualization tools can make this process manageable. We emphasize the critical importance of involving domain experts in data curation using intuitive technologies they can readily adopt. Manual and collaborative data cleaning yields significant ML performance gains, whereas blind reliance on automated filtering strategies may prove counterproductive.

Funding Disclosure

LS and RSW were supported by a Google Research award for "Peat-ML2: A new global benchmark for global peatland carbon inventories", awarded to JRM and RSW.

References

Aroyo, L. *et al.* (2022) "Data excellence for AI," *Interactions*, 29(2), pp. 66–69.

Austin, K.G. *et al.* (2025) "Mismatch between global importance of peatlands and the extent of their protection," *Conserv. Lett.*, 18(1).

Batjes, N.H., Ribeiro, E. and Oostrum, A. van (2020) "Standardised soil profile data to support global mapping and modelling (WoSIS snapshot 2019)," *Earth Syst. Sci. Data*, 12(1), pp. 299–320.

Böken, B. (2021) "On the appropriateness of platt scaling in classifier calibration," *Information Systems*, 95, p. 101641.

Cha, S. *et al.* (2024) "Unveiling the past: Deep-learning-based estimation of historical peatland distribution," *Land (Basel)*, 13(3), p. 328.

Dargie, G.C. *et al.* (2017) "Age, extent and carbon storage of the central congo basin peatland complex," *Nature*, 542(7639), pp. 86–90.

Dreschel, T.W. *et al.* (2017) "Peat soils of the everglades of florida, USA," in *Peat*. IntechOpen.

Ester, M. *et al.* (1996) "A density-based algorithm for discovering clusters in large spatial databases with noise," in *Proceedings of the second international conference on knowledge discovery and data mining (KDD'96)*. Portland, OR: AAAI Press, pp. 226–231.

Fiantis, D. *et al.* (2023) "Mapping peat thickness and carbon stock of a degraded peatland in west sumatra, indonesia," *Soil Use Manag.* [Preprint].

Florek, P. and Zagdański, A. (2023) "Benchmarking state-of-the-art gradient boosting algorithms for classification," *preprint: arXiv:2305.17094* [Preprint].

Fluet-Chouinard, E. *et al.* (2023) "Extensive global wetland loss over the past three centuries," *Nature*, 614(7947), pp. 281–286. Available at: https://doi.org/10.1038/s41586-022-05572-6.

Girkin, N.T. *et al.* (2022) "Tropical peatlands in the anthropocene: The present and the future," *Anthropocene*, 40(100354), p. 100354.

Gorham, E. (1991) "Northern peatlands: Role in the carbon cycle and probable responses to climatic warming," *Ecological applications*, 1(2), pp. 182–195.

Hastie, A. *et al.* (2024) "A new data-driven map predicts substantial undocumented peatland areas in amazonia," *Environ. Res. Lett.*, 19(9), p. 094019.

Hugelius, G. *et al.* (2020) "Large stocks of peatland carbon and nitrogen are vulnerable to per-

mafrost thaw," *Proceedings of the National Academy of Sciences*, 117(34), pp. 20438–20446. Available at: https://doi.org/10.1073/pnas.1916387117.

Ivanovs, J., Haberl, A. and Melniks, R. (2024) "Modeling geospatial distribution of peat layer thickness using machine learning and aerial laser scanning data," *Land*, 13(4). Available at: https://doi.org/10.3390/land13040466.

Jackson, R.B. *et al.* (2017) "The ecology of soil carbon: Pools, vulnerabilities, and biotic and abiotic controls," *Annual Review of Ecology, Evolution, and Systematics*, 48(1), pp. 419–445. Available at: https://doi.org/10.1146/annurev-ecolsys-112414-054234.

Jemeljanova, M., Kmoch, A. and Uuemaa, E. (2024) "Adapting machine learning for environmental spatial data - a review," *Ecol. Inform.*, 81(102634), p. 102634.

Joosten, H. and Clarke, D. (2002) *Wise use of mires and peatlands*. International Mire Conservation Group; International Peat Society.

Ke, G. *et al.* (2017) "Lightgbm: A highly efficient gradient boosting decision tree," *Advances in neural information processing systems*, 30.

Lara, M.J. *et al.* (2025) "A 20 m spatial resolution peatland extent map of alaska," *Sci. Data*, 12(1), p. 226.

Li, C. *et al.* (2018) "Erosion in peatlands: Recent research progress and future directions," *Earth-science reviews*, 185, pp. 870–886. Available at: https://doi.org/10.1016/j.earscirev.2018.08.005.

Li, P. *et al.* (2021) "CleanML: A study for evaluating the impact of data cleaning on ML classification tasks," in *2021 IEEE 37th international conference on data engineering (ICDE)*. IEEE, pp. 13–24.

Melton, J.R. *et al.* (2022) "A map of global peatland extent created using machine learning (peat-ML)," *Geoscientific Model Development Discussions*, 2022, pp. 1–44.

Minasny, B. *et al.* (2019) "Digital mapping of peatlands–a critical review," *Earth-Science Reviews*, 196, p. 102870.

Minasny, B. *et al.* (2023) "Mapping and monitoring peatland conditions from global to field scale," *Biogeochemistry*, 167(4), pp. 383–425.

Moran, P.A.P. (1950) "Notes on continuous stochastic phenomena," *Biometrika*, 37(1/2), pp. 17–23. Available at: https://doi.org/10.2307/2332142.

Musthofa, F. *et al.* (2022) "Machine learning for mapping spatial distribution of thickness and carbon stock of tropical peatland based on remote sensing data: A case study in lake sentarum national park, indonesia," *Geogr. Tech.*, 17(1/2022), pp. 46–57.

Niculescu-Mizil, A. and Caruana, R. (2005) "Predicting good probabilities with supervised learning," in *Proceedings of the 22nd international conference on machine learning*, pp. 625–632.

Pan, Z. *et al.* (2025) "Detecting and mapping peatlands in the tibetan plateau region using the random forest algorithm and sentinel imagery," *Remote Sens. (Basel)*, 17(2), p. 292.

Poggio, L. *et al.* (2021) "SoilGrids 2.0: Producing soil information for the globe with quantified spatial uncertainty," *Soil* [Preprint].

Pohjankukka, J. *et al.* (2025) "Digital mapping of peat thickness and extent in finland using remote sensing and machine learning," *Geoderma*, 455(117216), p. 117216.

Pontone, N. *et al.* (2024) "A hierarchical, multi-sensor framework for peatland sub-class and vegetation mapping throughout the canadian boreal forest," *Remote Sens. Ecol. Conserv.*, 10(4), pp. 500–516.

Roberts, D.R. *et al.* (2017) "Cross-validation strategies for data with temporal, spatial, hierarchical, or phylogenetic structure," *Ecography (Cop.)*, 40(8), pp. 913–929.

Roscher, R. *et al.* (2024) "Better, not just more: Data-centric machine learning for earth observation," *IEEE Geosci. Remote Sens. Mag.*, 12(4), pp. 335–355.

Sarracino, F. and Mikucka, M. (2017) "Bias and efficiency loss in regression estimates due to duplicated observations: A monte carlo simulation," *SRM* [Preprint].

Scottish Government (2025) "Peatland action – peat depth point data." Scotland's Soils (Scotland, UK). Available at: https://soils.environment.gov.scot/maps/point-data/peatland-action-peat-depth/ (Accessed: June 25, 2025).

Skye, Jade, Melton, J., *et al.* (2025) "Peat-DBase v.1: A compiled database of global peat depth measurements." Zenodo. Available at: https://doi.org/10.5281/ZENODO.16384775.

Skye, J. *et al.* (2025) "Peat-DBase v.1: A compiled database of global peat depth measurements," *Earth System Science Data Discussions*, 2025, pp. 1–26. Available at: https://doi.org/10.5194/essd-2025-432.

Skye, Jade, Melton, J.R., *et al.* (2025) "PeatDepth-ML: A global map of peat depth predicted using machine learning," *EGUsphere*, 2025, pp. 1–39. Available at: https://doi.org/10.5194/egusphere-2025-5363.

Treat, C.C. *et al.* (2017) "(Table S2) global dataset of peatland basal ages." PANGAEA - Data Publisher for Earth & Environmental Science. Available at: https://doi.org/10.1594/PANGAEA.873065.

Turek, M.E. *et al.* (2023) "Global mapping of volumetric water retention at 100, 330 and 15 000

cm suction using the WoSIS database," *Int. Soil Water Conserv. Res.*, 11(2), pp. 225–239.

Turetsky, M.R. *et al.* (2015) "Global vulnerability of peatlands to fire and carbon loss," *Nature Geoscience*, 8(1), pp. 11–14.

Unep (2022) "Global peatlands Assessment–The state of the world's peatlands: Evidence for action toward the conservation, restoration, and sustainable management …," *Main Report. Global Peatlands Initiative* [Preprint].

Wadoux, A.M.J.-C., Minasny, B. and McBratney, A.B. (2020) "Machine learning for digital soil mapping: Applications, challenges and suggested solutions," *Earth Sci. Rev.*, 210(103359), p. 103359.

Widyastuti, M.T. *et al.* (2025) "Digital mapping of peat thickness and carbon stock of global peatlands," *CATENA*, 258, p. 109243. Available at: https://doi.org/10.1016/j.catena.2025.109243.

Winton, R.S. *et al.* (2025) "Widespread carbon-dense peatlands in the colombian lowlands," *Environ. Res. Lett.*, 20(5), p. 054025.

Xu, J. *et al.* (2018) "PEATMAP: Refining estimates of global peatland distribution based on a meta-analysis," *Catena*, 160, pp. 134–140. Available at: https://doi.org/10.1016/j.catena.2017.09.010.

Zanaga, D. *et al.* (2022) "ESA WorldCover 10 m 2021 v200." Zenodo. Available at: https://doi.org/10.5281/zenodo.7254221.

Appendix

A Geographical Clusters Filtering

Uneven sampling distributions can bias ML models toward densely sampled regions, making it crucial to address geographic sampling imbalances during training. To ensure more equitable representation, measurements from sparsely sampled regions should carry greater weight than those from well-represented areas. We address this issue by applying the DBSCAN clustering algorithm (Ester *et al.*, 1996) to group peat data points into geographical clusters, then using these clusters to weight the loss function during model training.

DBSCAN parameters of $\epsilon = 0.3$ and minimum samples = 5 produced 12 initial clusters. Through visual inspection, we consolidated these into 7 final clusters while excluding 30 outlier datapoints. Appendix Figure 1 displays the resulting cluster distribution, with data point counts provided in Appendix Table 1.

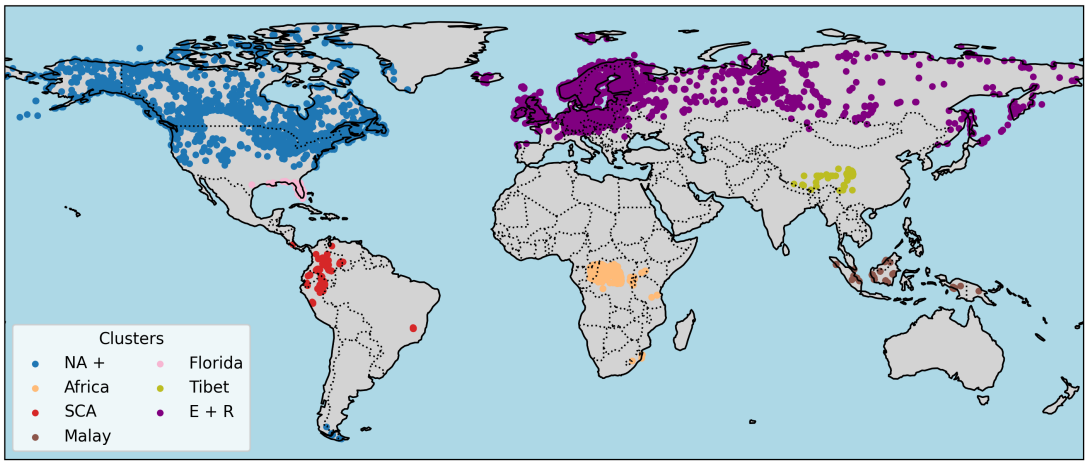

Appendix Figure 1: Clustered Peat Measurements Map. The clusters' abbreviated names designate the following regions: NA+: North American plus Southern Chile; Africa: African Continent; SCA: South and Central America; Malay: Malay Archipelago; Florida: Florida plus other states bordering the Gulf of Mexico; Tibet: Tibetan Highlands; and E+R: Europe plus Russia.

Appendix Table 1: Number of data points per peat-study cluster.

Region Name	Short Name	Data Points
Florida	Florida	64
Tibet	Tibet	135
Africa	Africa	1631
South and Central America	SCA	564
Malay Archipelago	Malay	388
North America + Southern Chile	NA +	25615
Europe and Russia	E + R	4309

Appendix Table 2: Number of data points per non-peat-study cluster.

Landcover Type	Data Points
Snow, Bare and Moss	2266
Mangrove	441
Herbaceous wetland	447
Permanent water bodies	682
Built-up	2187
Cropland	21888
Grassland	26352
Shrubland	6088
Tree cover	27185

For non-peat data points from the WoSIS database, we adopted a different clustering approach. Since these data points were already selected to span diverse geographical locations, we instead clustered them by landcover type to prevent model bias toward common landcover classes such as forests or grasslands. We classified data points using the ESA WorldCover 10m v200 product accessed through Google Earth Engine (Zanaga *et al.*, 2022). Appendix Table 2 presents the resulting distribution. We combined the "Snow and Ice," "Bare and sparse vegetation," and "Moss and lichen" categories due to their limited sample sizes and similarities with regards to vegetation.

B Machine-Learning Model

B.1 LightGBM Model

To determine peat presence on a global 5 arc-minute grid, we employ LightGBM (Ke *et al.*, 2017), following the approach of (Melton *et al.*, 2022). This gradient-boosting algorithm uses histogram-based methods and leaf-wise tree growth to achieve faster training than traditional boosting methods while maintaining state-of-the-art performance comparable to Random Forests. The model takes environmental predictors as inputs, uses gridded peat soil cores as ground truth, and outputs probabilities for peat presence in each cell.

Gradient-boosting methods used for binary classification problems train models by minimizing the binary cross-entropy loss function, which itself is the negative log likelihood of the Bernouilli distribution. We modify this loss function with non-uniform weights to account for the sampling bias of our data points. Taking N to be the total number of data points after filtering, we assign $N/2$ as the sum of weights for both peat-study and non-peat-study samples. Then, for the peat-study samples, we divide $N/2$ by the number of clusters to assign a total weight for each cluster. Finally, within each cluster, we divide the cluster weight by the number of data points in that cluster to determine individual weights. We do the same for the non-peat-study data. If we let C_p and C_n be the number of peat-study and non-peat-study clusters, respectively, and if n_i is the number of data points in cluster $i \in \{-C_n + 1, \dots, 0, \dots, C_p\}$ (ordering the non-peat-study

clusters from $-C_n + 1$ to 0 and the peat-study clusters from 1 to C_p), then the sample weight of data point j in cluster i is determined by:

$$\omega_j^i = \frac{N}{2} \frac{1}{C_k} \frac{1}{n_i}$$

where $k = p$ if $i > 0$ and $k = n$ else. Then, once the individual sample weights are computed, we assign the grid cell weights as follows:

$$\text{For each grid cell:} \begin{cases} \text{If there is at least one peat-study data point:} \\ \quad \text{Peat presence} = 1 \\ \quad \text{Cell weight} = \sum \text{weights of all peat-study data points} \\ \text{If there are no peat-study data points:} \\ \quad \text{Peat presence} = 0 \\ \quad \text{Cell weight} = \sum \text{weights of all non-peat-study data points} \end{cases}$$

This approach maintains approximate weight balance between peat-study and non-peat-study cells, effectively addressing sampling bias while accommodating the spatial aggregation to grid cells.

We use the following hyperparameters: maximum leaves = 31, estimators = 1000, learning rate = 0.01, with remaining parameters at default values. Since this study focuses on data curation effects rather than model optimization, we do not perform hyperparameter tuning.

B.2 Predictor Selection

We begin with 399 predictors and apply a systematic filtering process. First, we remove 31 near-constant predictors using a variance cutoff of 10^{-4}. Next, we eliminate 206 highly correlated predictors by removing variables with correlation coefficients above 0.95 (or below -0.95), retaining only one predictor from each correlated pair and yielding 162 predictors.

We then train LightGBM on the raw data using these 162 predictors and select the 20 variables with the highest feature importance gains. The resulting predictors are displayed in Appendix Table 3.

A single predictor value is thus obtained for every grid cell. LightGBM can handle NaN values natively and thus we do not remove them prior to training.

Appendix Table 3: Top 20 predictors used in the initial LightGBM run. GEE stands for Google Earth Engine.

Predictor	Source
Annual mean climatic water deficit	GEE: IDAHO_EPSCOR/TERRACLIMATE
Climatic water deficit over Sept–Oct–Nov	GEE: IDAHO_EPSCOR/TERRACLIMATE
Actual evapotranspiration over June–July–Aug	GEE: IDAHO_EPSCOR/TERRACLIMATE
Topsoil clay fraction (0–5 cm)	GEE: OpenLandMap
Geomorphon classification	Geomorpho90m; https://doi.pangaea.de/10.1594/PANGAEA.899135
Vapor pressure deficit over Sept–Oct–Nov	GEE: IDAHO_EPSCOR/TERRACLIMATE
Solar radiation over Dec–Jan–Feb	GEE: IDAHO_EPSCOR/TERRACLIMATE
Solar radiation over June–July–Aug	GEE: IDAHO_EPSCOR/TERRACLIMATE
Growing season temperature	CHELSA-BIOCLIM+; https://doi.org/10.16904/envidat.332
Climatic water deficit over June–July–Aug	GEE: IDAHO_EPSCOR/TERRACLIMATE
Palmer Drought Severity Index over June–July–Aug	GEE: IDAHO_EPSCOR/TERRACLIMATE
Length of longest day of year	Computed from latitude
Roughness magnitude	Geomorpho90m; https://doi.pangaea.de/10.1594/PANGAEA.899135
Temperature seasonality	WorldClim 2 Bioclimatic Variables; https://doi.org/10.1002/joc.5086
Soil moisture over Dec–Jan–Feb	GEE: IDAHO_EPSCOR/TERRACLIMATE
Vegetation water content	GEE: NASA/SMAP/SPL3SMP_E/005
Palmer Drought Severity Index over Dec–Jan–Feb	GEE: IDAHO_EPSCOR/TERRACLIMATE
Topsoil bulk density (0–5 cm)	GEE: OpenLandMap
Photosynthetically active radiation in June–July–Aug	GEE: MODIS Terra + Aqua
Red band reflectance average over March–April–May	GEE: NASA/VIIRS/002/VNP13A1

B.3 Validation

In order to account for the spatial autocorrelation of our geospatial dataset and provide reasonable performance estimates on new data, we employ a Blocked-Leave-One-Out Cross Validation (BLOO CV) strategy (Roberts *et al.*, 2017; Jemeljanova, Kmoch and Uuemaa, 2024) similar to the one used in (Melton *et al.*, 2022). We calculate the Moran's I index (Moran, 1950) for our model's residuals with increasing spatial-lag distances and determine that a distance of approximately 6 degrees is sufficient for the MI index to settle near zero, indicating the end of the spatial autocorrelation regime (not shown).

A reasonable BLOO CV strategy selects blocks that slice the Earth North-South in sections of at least 6 degrees longitude while ensuring roughly equal data points per block. Data within each block is withheld from training and used as a validation set. This process is repeated for all blocks to obtain predictions covering the entire planet, ensuring the ML models never train on data they are predicting.

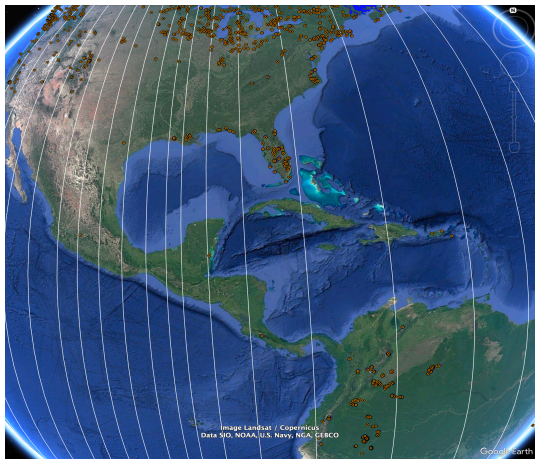

Appendix Figure 2: Staggered Block-Leave-One-Out Cross-Validation (SBLOO CV)

One limitation of this approach is its tendency to produce overly pessimistic performance estimates (Jemeljanova, Kmoch and Uuemaa, 2024). This is particularly problematic given our limited tropical data, where peatland ecosystems differ substantially from boreal peatlands (Unep, 2022). To generate more realistic performance assessments while maintaining spatial blocking, we employ a Staggered Block-Leave-One-Out Cross-Validation strategy (SBLOO CV).

We first reorganize the data into smaller blocks spanning a minimum of 2 degrees with roughly equal peat core counts. Then, we combine 3 consecutive smaller blocks to form each larger BLOO CV block (ensuring minimum 6-degree coverage). This process is repeated for all combinations of 3 consecutive smaller blocks, generating 3 different predictions per datapoint, which we average to obtain performance estimates. These smaller blocks are illustrated in Figure 2.

The SBLOO CV procedure improved performance for most smaller clusters, suggesting that standard BLOO CV may be overly conservative as suggested by (Jemeljanova, Kmoch and Uuemaa, 2024). As shown in Figure 11, Florida remains the only cluster with poor ML model performance.

Most Florida points are concentrated within a single smaller block (Figure 2), due to the region's predominantely North-South orientation, meaning this data is never observed during algorithm training. The poor Florida performance can therefore likely be attributed to an artifact of the SBLOO CV method rather than true model limitations.

B.4 Calibration

ML model probability outputs are often poorly calibrated (Niculescu-Mizil and Caruana, 2005). To address this issue, we use the SBLOO CV validation sets described above to calibrate model probabilities. We employ Platt Scaling, a simple yet effective technique that fits a logistic regression model using raw model outputs as features and validation set ground truth as targets (Böken, 2021).

B.5 Thresholding

Our ML model aims to identify peat presence on a coarse grid, with peat-study cells subsequently examined in detail at finer resolutions. As mentioned earlier, we prioritize detecting the vast majority of peatlands over minimizing false positives, as high recall is more important than high precision for our approach.

Consequently, we can select probability thresholds significantly below 50% for classifying model outputs. Using the validation set, we determine the threshold that optimizes the trade-off between recall and precision. Details are presented in Section 3.1.1.

C Comparison with another set of predictors

This appendix contains the simulated results for another set of predictors, for comparison. These predictors were handpicked as 20 top predictors from previous work (Melton *et al.*, 2022; Jade Skye, J. R. Melton, *et al.*, 2025). They are displayed in Table 4.

The results obtained by applying various combinations of filters are displayed in the 4 tables below.

Appendix Table 4: Alternative set of top predictors used as a test. GEE stands for Google Earth Engine.

Predictor	Source
Runoff over Sept–Oct–Nov	GEE: IDAHO_EPSCOR/TERRACLIMATE
Annual mean vapour pressure deficit	GEE: IDAHO_EPSCOR/TERRACLIMATE
Greenup date (first greenup)	GEE: MODIS/061/MOD17A3HGF
Terrain slope	Geomorpho90m; https://doi.pangaea.de/10.1594/PANGAEA.899135
10 m wind speed over March–April–May	GEE: IDAHO_EPSCOR/TERRACLIMATE
Vapour pressure deficit over Sept–Oct–Nov	GEE: IDAHO_EPSCOR/TERRACLIMATE
Tangential curvature	Geomorpho90m; https://doi.pangaea.de/10.1594/PANGAEA.899135
Snow water equivalent over Dec–Jan–Feb	GEE: IDAHO_EPSCOR/TERRACLIMATE
Solar radiation over March–April–May	GEE: IDAHO_EPSCOR/TERRACLIMATE
Soil moisture over Sept–Oct–Nov	GEE: IDAHO_EPSCOR/TERRACLIMATE
Roughness magnitude	Geomorpho90m; https://doi.pangaea.de/10.1594/PANGAEA.899135
SWIR3 mean reflectance (2225–2275 nm)	GEE: NASA/VIIRS/002/VNP13A1
Runoff over March–April–May	GEE: IDAHO_EPSCOR/TERRACLIMATE
Runoff over June–July–Aug	GEE: IDAHO_EPSCOR/TERRACLIMATE
Palmer Drought Severity Index over Sept–Oct–Nov	GEE: IDAHO_EPSCOR/TERRACLIMATE
Minimum annual Net Primary Productivity across years	GEE: MODIS/061/MOD17A3HGF
Maximum annual Net Primary Productivity across years	GEE: MODIS/061/MOD17A3HGF
Geomorphon landform class	Geomorpho90m; https://doi.pangaea.de/10.1594/PANGAEA.899135
Second senescence date (late-season senescence)	GEE: MODIS/061/MCD12Q2
Year exposed from ice and sea	Calculated; https://doi.org/10.1038/s41467-021-21469-w

Appendix Table 5: Comparison of classification performance metrics (Accuracy, Precision, Recall, F1) across different types of precision filters for another set of predictors.

Filtering	Accuracy	Precision	Recall	F1 Score
Baseline	0.888	0.499	0.887	0.639
AND - 0	0.889	0.501	0.889	0.641
OR - 0	0.891	0.5	0.891	0.64
AND - 1	0.89	0.499	0.891	0.64
OR - 1	0.894	0.489	0.893	0.632
AND - 2	0.906	0.514	0.906	0.656
OR - 2	0.901	0.472	0.9	0.619
AND - 3	0.895	0.411	0.898	0.564
OR - 3	0.89	0.372	0.888	0.524

Appendix Table 6: False negative rate (% of peat points missed) per peat-study cluster across filtering strategies for another set of predictors.

Filtering	Florida	Tibet	Africa	SA	Malay Archipelago	NA +	Europe and Russia
Baseline	51.79	60.98	55.07	8.40	34.48	13.68	4.84
AND - 0	50.00	62.20	62.32	8.47	31.03	13.37	4.54
OR - 0	53.57	55.00	48.53	7.83	25.93	13.44	4.62
AND - 1	50.00	59.49	59.70	8.47	31.03	13.22	4.64
OR - 1	50.00	66.13	45.00	6.19	32.00	13.24	4.52
AND - 2	48.21	64.86	57.58	7.89	25.00	10.57	3.99
OR - 2	55.36	76.92	43.10	3.64	39.13	11.78	4.18
AND - 3	39.29	72.97	45.45	3.92	21.43	10.85	4.08
OR - 3	18.87	84.31	41.38	3.96	34.78	12.89	5.04

Appendix Table 7: False positive rate (% of zero-depth peat points incorrectly predicted as peat) per non-peat-study cluster across filtering strategies for another set of predictors.

Filtering	Bare	Mangrove	Wetland	Water	Urban	Crop	Grass	Shrub	Tree
Baseline	10.26	7.26	18.57	34.93	9.95	6.86	7.59	1.12	19.83
AND - 0	10.35	8.11	16.09	35.66	9.87	6.91	7.85	1.02	19.48
OR - 0	9.86	8.70	17.26	35.92	9.91	7.05	7.63	0.97	18.92
AND - 1	10.60	8.15	18.18	37.73	9.77	6.67	7.65	0.98	19.68
OR - 1	9.24	8.20	16.42	36.14	10.45	7.09	7.30	0.89	18.89
AND - 2	5.98	6.08	16.35	29.94	10.53	7.32	6.99	0.60	15.78
OR - 2	6.39	5.33	15.48	27.86	11.69	7.48	7.62	0.83	16.33
AND - 3	6.64	6.49	17.62	29.21	12.79	7.90	7.64	0.58	17.60
OR - 3	6.14	6.51	18.45	29.66	13.81	7.70	8.41	0.85	18.86

Appendix Table 8: Comparison of classification performance metrics (Accuracy, Precision, Recall, F1) across different filtering strategies for another set of predictors, as presented in Appendix Table 4.

Filtering	Accuracy	Precision	Recall	F1 Score
none	0.888	0.499	0.887	0.639
landcover-auto	0.894	0.479	0.895	0.624
landcover-manual	0.889	0.493	0.889	0.634
AND-2	0.906	0.514	0.906	0.656
AND-2 + landcover-auto	0.910	0.501	0.909	0.646
AND-2 + landcover-manual	0.910	0.523	0.912	0.665

D Test with DMS filtering

Here we present results collected by applying a Degrees/Minutes/Seconds (DMS) filter to the dataset prior to training the ML model. We converted all points to DMS - accounting for possible truncated decimal expansions in performing the conversion (e.g. 41.333333° becomes 41°20′00 and not 41°19′59.9988) - and then removed the points with low precision in DMS, i.e. points that only have non-zero degrees and minutes, but no recorded seconds, in both latitude and longitude (DMS-AND-seconds filter). We tested a variety of combinations and display some of them in Table 9.

Appendix Table 9: Comparison of classification performance metrics (Accuracy, Precision, Recall, F1) across different filtering strategies with the DMS filter.

Filtering	Accuracy	Precision	Recall	F1 Score
none	0.899	0.527	0.900	0.664
DMS-AND-seconds	0.901	0.521	0.901	0.661
AND-2 + DMS-AND-seconds	0.911	0.529	0.909	0.669
AND-2 + DMS-AND-seconds +landcover-auto	0.901	0.521	0.901	0.661
AND-2 + DMS-AND-seconds +landcover-manual	0.914	0.533	0.916	0.674
AND-2 + landcover-manual	0.918	0.548	0.917	0.686